Magnetic characteristics of CV chondrules with paleointensity implications

Stacey Emmerton,[1] Adrian R. Muxworthy,[1] Dominik C. Hezel,[2,3] and Philip A. Bland[1,2,4]

Received 4 May 2011; revised 25 October 2011; accepted 26 October 2011; published 29 December 2011.

[1] We have conducted a detailed magnetic study on 45 chondrules from two carbonaceous chondrites of the CV type: (1) Mokoia and (2) Allende. Allende has been previously extensively studied and is thought to have a high potential of retaining an extra-terrestrial paleofield. Few paleomagnetic studies of Mokoia have previously been undertaken. We report a range of magnetic measurements including hysteresis, first-order reversal curve analysis (FORCs), demagnetization characteristics, and isothermal remanent (IRM) acquisition behavior on both Mokoia and Allende chondrules. The Mokoia chondrules displayed more single domain-like behavior than the Allende chondrules, suggesting smaller grain sizes and higher magnetic stability. The Mokoia chondrules also had higher average concentrations of magnetic minerals and a larger range of magnetic characteristics than the Allende chondrules. IRM acquisition analysis found that both sets of chondrules have the same dominant magnetic mineral, likely to be a FeNi phase (taenite, kamacite, and/or awaruite) contributing to 48% of the Mokoia chondrules and 42% of the Allende chondrule characteristics. FORC analysis revealed that generally the Allende chondrules displayed low-field coercivity distributions with little interactions, and the Mokoia chondrules show clear single-domain like distributions. Paleointensity estimates for the two meteorites using the REMc and Preisach methods yielded estimates between 13 and 60 μT and 3–56 μT, respectively, for Allende and 3–140 μT and 1–110 μT, respectively, for Mokoia. From the data, we suggest that Mokoia chondrules carry a non-primary remagnetization, and while Allende is more likely than Mokoia to retain its primary magnetization, it also displays signs of post accretionary magnetization.

Citation: Emmerton, S., A. R. Muxworthy, D. C. Hezel, and P. A. Bland (2011), Magnetic characteristics of CV chondrules with paleointensity implications, *J. Geophys. Res.*, *116*, E12007, doi:10.1029/2011JE003856.

1. Introduction

[2] Knowledge of magnetic fields within the solar nebula is important for our understanding of the formation of the solar system. The only direct methods to estimate nebula magnetic fields is to determine ancient magnetic field intensities (paleofield intensities or paleointensities) potentially recorded by magnetic iron and iron-nickel bearing meteorites formed in the early solar nebula [*Collinson*, 1994; *Weiss et al.*, 2010] or by direct detection of the magnetic fields in accretion disks [*Donati et al.*, 2005]. Carbonaceous chondrites are likely to be the most reliable recorders as they are undifferentiated stony meteorites containing four individual components: chondrules (20–80 vol%), matrix (20%–80%), CAIs (calcium-Aluminum Inclusions) (0–3 vol%), and metal/sulphides (0–8 vol%) [*Brearley and Jones*, 1998; *Zanda*, 2004; *Huss et al.*, 2005; *Hezel et al.*, 2008]. The chondrules can potentially record the primitive magnetic field because they formed 4.56 billion years ago during rapid cooling (minutes to hours) from above their respective melting temperature (up to 2000 K) allowing them to record a primitive thermoremanence (TRM) before the chondritic meteorites accreted [*Sugiura et al.*, 1979; *Sears*, 2004]. The magnetic signal is thought to be carried by metallic-iron, FeNi or iron oxides and sulphides [*Weiss et al.*, 2010]. However, given the long and often complex formation history of chondrules, opinion is divided as to whether the remanence carried by chondrules is primitive (i.e., nebula) or secondary (i.e., asteroidal) in origin [*Acton et al.*, 2007].

[3] Even though there are uncertainties as to the origin of the magnetic remanence, recovering paleofield estimates from meteorites has been an area of study for decades [*Stacey*, 1976; *Lanoix et al.*, 1978; *Wasilewski*, 1981; *Acton et al.*, 2007]. Earlier studies typically employed heating

---

[1] Impacts and Astromaterials Research Centre, Department of Earth Science and Engineering, Imperial College London, London, UK.

[2] Impacts and Astromaterials Research Centre, Department of Mineralogy, Natural History Museum, London, UK.

[3] Department of Geology and Mineralogy, University of Cologne, Cologne, Germany.

[4] Department of Applied Geology, Curtin University of Technology, Perth, Western Australia, Australia.

Table 1. Summary of Measurements Taken for Each Sample in This Study

	Magnetic Properties					Hysteresis Properties				Paleointensity Proxies	
Sample	Mass (mg)	NRM (mAm^2/kg)	SIRM (mAm^2/kg)	SIRMMDF (mT)	ChRM Interval (mT)	H$_{cr}$ (mT)	H$_c$ (mT)	M$_{rs}$/M$_s$	FORC Class	REMc (μT)	Preisach (μT)
Allende2	2.20	3.7	9.4	54	40–70	34.6	8.5	0.09	MA	57 ± 16	···
Allende5	0.20	0.3	3.5	30	···	36.9	11.8	0.12	A	···	···
Allende6	1.70	0.2	21.3	67	50–80	41.6	5.5	0.06	A	21 ± 2	22 ± 1
Allende10	0.90	0.4	20.5	62	20–40	42.1	10.4	0.11		25 ± 5	39 ± 1
Allende21	0.90	0.1	37.1	25	40–70	78.2	18.2	0.15		30 ± 4	···
Allende30	0.60	0.3	46.2	47	15–70	75.0	12.5	0.11		15 ± 6	5 ± 1
Allende36	0.26	0.3	1.4	57	12–50	36.0	9.9	0.09	A	···	···
Allende44	1.20	2.1	44.6	24	20–70	33.3	11.9	0.10	MA	20 ± 8	···
Allende49	0.27	0.1	3.9	23	···	38.9	8.6	0.08	A	···	···
Allende66	0.37	0.1	14.7	25	···	57.0	11.2	0.09	A	···	···
Allende67	0.28	0.6	104.5	20	15–40	61.4	12.6	0.10	A$_1$	39 ± 4	56 ± 4
Allende68	0.30	0.5	49.3	21	10–25	38.9	8.6	0.08	MA	14 ± 5	11 ± 2
Allende69	0.56	0.2	13.1	23	···	43.7	10.7	0.11	A	···	···
Allende70	1.45	0.3	27.0	25	40–77	26.3	11.0	0.14	A$_1$	30 ± 4	13 ± 4
Allende72	0.98	0.7	38.9	26	30–90	19.5	7.4	0.20	MA	18 ± 8	
Allende73	0.86	0.2	99.9	28	40–80	34.4	9.6	0.09	A$_1$	13 ± 4	3 ± 1
Allende76	0.54	0.4	6.1	24	15–25	33.8	9.1	0.09	A	60 ± 3	···
Mokoia14	0.85	2.3	41.7	22	15–50	36.1	17.6	0.24	M	8 ± 6	···
Mokoia28	0.60	1.2	38.7	28	12–60	38.8	18.3	0.23		77 ± 3	17 ± 1
Mokoia29	0.75	1.7	50.3	27	20–60	39.5	18.1	0.21	M	77 ± 3	21 ± 3
Mokoia33	0.50	4.8	48.2	20	25–50	42.8	11.3	0.10	M	140 ± 26	…
Mokoia34	0.65	4.8	62.5	24	30–60	45.1	27.4	0.34	M	49 ± 8	…
Mokoia35	1.00	2.4	7.0	23	···	30.4	19.5	0.29	MA	···	···
Mokoia37	1.20	67.1	120	18	15–70	39.6	4.0	0.02	M	11 ± 4	…
Mokoia52	0.80	1.4	38.1	30	15–40	33.0	17.4	0.22	M	85 ± 4	47 ± 9
Mokoia56	0.85	0.8	53.1	23	9–35	40.2	21.4	0.26	M	22 ± 2	110 ± 6
Mokoia58	1.30	1.2	53.9	20	···	35.0	13.3	0.14	M	···	···
Mokoia59	1.40	0.2	19.1	23	···	35.4	15.0	0.17	M	···	···
Mokoia62	0.85	1.6	41.1	25	15–30	38.7	23.0	0.30	M	72 ± 10	26 ± 1
Mokoia67	0.76	0.7	21.2	30	12–40	37.2	14.7	0.17	M	88 ± 4	68 ± 6
Mokoia68	0.64	0.7	63.3	25	12–50	89.2	40.1	0.39	M	36 ± 3	16 ± 1
Mokoia76	2.47	8.4	940	24	···	40.9	20.1	0.17		···	···
Mokoia77	0.73	0.2	234	25	15–65	46.7	24.2	0.31	M	3 ± 2	1 ± 0.1
Mokoia78	1.05	0.2	46.8	33	15–60	56.5	30.2	0.32	M	15 ± 3	3 ± 0.3
Mokoia79	0.73	0.3	79.2	26	···	38.1	21.5	0.27	MA	···	···
Mokoia80	0.97	5.1	329	25	15–70	42.1	21.4	0.19	M	7 ± 5	…
Mokoia81	0.54	11.1	633	22	10–40	42.1	24.2	0.32	M	6 ± 2	…
Mokoia82	1.00	0.2	435	30	···	40.3	18.2	0.22	M	···	···
Mokoia83	0.58	3.3	1048	21	···	43.9	27.1	0.29	M	···	···
Mokoia84	0.61	0.1	73.9	39	···	56.6	24.6	0.26	M	···	···
Mokoia85	0.87	2.7	655	24	···	50.7	2.6	0.01	M	···	···
Mokoia86	0.32	0.2	96.8	23	···	44.5	22.2	0.24	M	···	···
Mokoia87	0.77	0.4	25.5	28	10–40	41.1	20.1	0.21		30 ± 5	29 ± 3
Mokoia88	0.33	0.7	96.0	24	10–50	40.6	21.7	0.25	M	12 ± 4	1 ± 0.2
Mokoia89	0.37	0.2	20.5	26	···	38.8	19.6	0.25		···	···
AllendeM1^a	1.00	1.2	121	71	50–90	82.6	29.4	0.19		22 ± 2	128 ± 9
AllendeM2^a	0.20	1.7	1.4	72	50–70	*^{b}	*	*		28 ± 2	···
Mokoia M^a	0.50	1.2	354	15	50–90	54.6	29.6	0.31	M	14 ± 6	···
Allende B^c	88.40	0.3	60.8	70	50–90	*	*	*		22 ± 1	···
Mokoia B^c	62.20	10.6	983	38	15–50	*	*	*		3 ± 2	···

[a] Matrix material.

[b] Sample too large to measure on AGM.

[c] Bulk material.

approaches such as modified Thellier-type method [*Thellier and Thellier*, 1959] yielding a wide range of values from 5–1600 μT, which are now generally thought to be unreliable due to the thermal instability of most chondrules [*Westphal*, 1986; *Jones et al.*, 2005]. *Yu et al.* [2009] proposed modifications to the Thellier protocol to potentially isolate a correct paleofield estimate. Alternative non-heating methods for determining paleofield intensities have been applied, in particular the REM method and its variations is one protocol that has been routinely applied to chondrules and other meteoritic material [e.g., *Kletetschka et al.*, 2003; *Gattacceca and Rochette*, 2004; *Acton et al.*, 2007]. *Gattacceca and Rochette* [2004] estimate an accuracy to at best a factor of two for this technique, but *Yu* [2006] suggests it could be worse.

[4] The aim of this paper is to investigate the magnetic remanence carried by chondrules in the CV-type carbonaceous chondrites, Mokoia and Allende. These meteorites were chosen because a variety of petrographic evidence indicates that they have not experienced significant shock pressures,

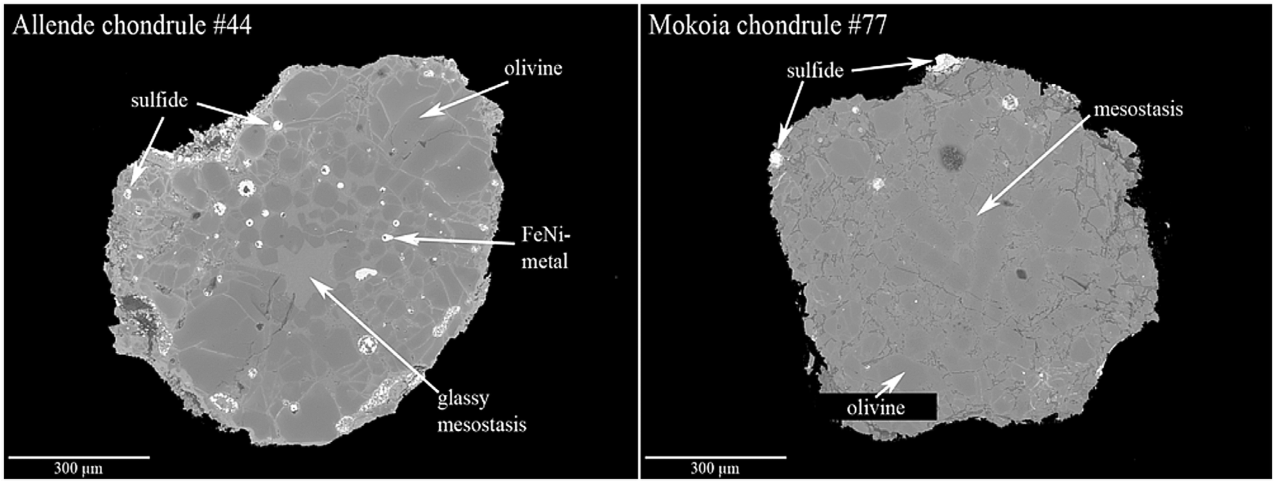

Figure 1. SEM images of chondrules in this study demonstrating the cleanliness of the samples. Chondrules from (left) Allende and (right) Mokoia.

hence the magnetic remanence is more likely to display only minor secondary modifications induced by shock relative to other meteorites. Both Mokoia and Allende are assigned to shock stage S1 [*Scott et al.*, 1992], consistent with shock pressures of <4–5 GPa, and mean shock-induced temperature increases of <100°C [*Scott et al.*, 1991, 1992; *Stöffler et al.*, 1991a, 1991b]. In the case of Allende, a detailed analysis by *Nakamura et al.* [1995] found that silicate minerals in many chondrules are unfractured and generally show sharp extinction. The mean aspect ratio of 26 chondrules is 1.09, indicating that chondrules are nearly spherical. In addition, there is no preferred orientation of chondrules, and metal and sulphide inclusions in many chondrules are also nearly spherical, suggesting that they have not experienced deformation after the formation of chondrules. *Nakamura et al.* [1995] concluded that all these observations indicate that Allende is almost free of natural shock effects, consistent with the observation of *Scott et al.* [1992], however, individual magnetic minerals that reside in chondrules such as pyrrhotite have been shown to be completely remagnetized at 2.8 GPa [*Rochette et al.*, 2001], and shock pressures as low as 1.5 GPa can induce a significant SRM [*Gattacceca et al.*, 2008]. This potential shock magnetization should be taken into account when selecting the range of remanences for paleointensity estimates.

[5] The specific characteristics of hydrothermal alteration differ between the two meteorites as is reflected in their assignment to two different oxidized subgroups, Allende (CV_{oxA} – Allende like) and Mokoia (CV_{oxB} – Bali-like) [*Krot et al.*, 2005]. CV_{oxB} chondrites have experienced replacement of primary minerals by secondary minerals (e.g., phyllosilicates, magnetite, and Fe, Ni-sulfides) through aqueous alteration at relatively low temperatures on the CV asteroidal body. CV_{oxA} chondrites, however, show iron-alkali metasomatism from fluid-assisted thermal metamorphism on the CV asteroidal body and observations such as inverse compositional zoning in secondary fayalites suggest CV_{oxA} chondrites were altered at higher temperatures than CV_{oxB} chondrites. In fact, the lithology of Mokoia is a complex breccia dominated by CV_{oxB} lithologies, but it also contains CV_{oxA} alterations [*Krot et al.*, 2005].

[6] Magnetically, Allende has been extensively studied [e.g., *Butler*, 1972; *Brecher and Arrhenius*, 1974; *Herndon et al.*, 1976; *Brecher*, 1977; *Lanoix et al.*, 1978; *Nagata*, 1979; *Wasilewski*, 1981; *Nagata and Funaki*, 1983; *Sugiura and Strangway*, 1985; *Wasilewski and Dickinson*, 2000; *Carporzen et al.*, 2011] and is used in this study for comparison and validity of the results of the relatively unstudied Mokoia meteorite [*Brecher and Arrhenius*, 1974; *Stacey*, 1976]. In previous paleointensity studies of the Allende meteorite and other CV chondrites, the primary magnetic minerals were identified as FeNi alloys, taenite, kamacite and awaruite [*Nagata and Funaki*, 1983; *Krot et al.*, 1998], magnetite and iron sulphide (pyrrhotite) [*Banerjee and Hargraves*, 1972]. *Sugiura et al.* [1979] reported that Allende chondrules pass the conglomerate test on a few chondrules (i.e., the chondrules retain a remanence acquired prior to accreting into the meteorite parent body) but others suggest the opposite [*Weiss et al.*, 2009; *Carporzen et al.*, 2011]. *Sugiura et al.* [1979] also reported a primary remanence in chondrules heated to 300°C, however it is generally agreed that the bulk magnetization for Allende is carried within the matrix and was acquired after accretion [*Nagata and Funaki*, 1983; *Sugiura and Strangway*, 1985; *Weiss et al.*, 2009]. *Stacey* [1976] investigated the magnetization of the Mokoia meteorite and considered the magnetization to be unstable and possibly terrestrially induced because its natural remanence was destroyed on heating to 200°C.

[7] We report a detailed rock magnetic investigation of the minerals, designed to identify the magnetic carriers and the likelihood of the magnetic remanence being primitive in origin. We also report the paleofield intensities, in addition to applying the non-heating REMc method for determining paleointensities, we also report paleofield estimates determined using a recently developed non-heating method based on first-order-reversal-curves (FORC) data [*Muxworthy and Heslop*, 2011]. The model is built on a thermally activated Preisach model [*Preisach*, 1935; *Muxworthy and Heslop*, 2011] for randomly orientated interacting single domain grains with uniaxial anisotropy. From studies on terrestrial historical lavas it has been demonstrated to be more accurate

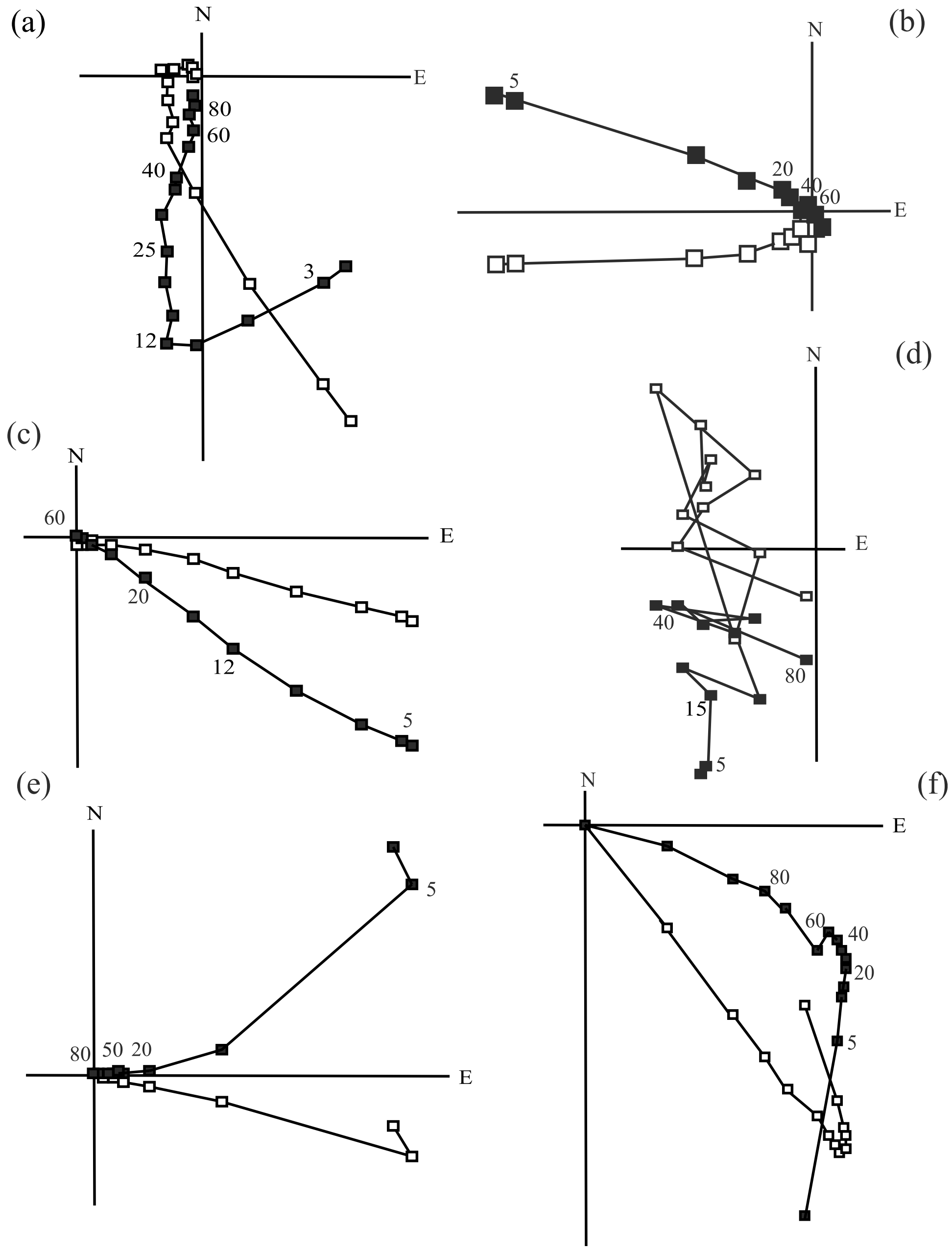

Figure 2. Representative Zijderveld plots for AF demagnetization of the NRM for (a) Mokoia28, (b) Allende44, (c) Mokoia33, and (d) Allende67. Both Mokoia and Allende chondrules typically show secondary magnetizations. Bulk samples for (e) Mokoia and (f) Allende also show two magnetization components. The field steps are marked on the plots in mT.

than the REM family of methods, and possibly as accurate as the Thellier method [*Muxworthy et al.*, 2011], but without the risk of alteration during heating.

2. Samples and Methodology

[8] We investigated a total of 45 chondrules from the two carbonaceous chondrites Mokoia (28 chondrules, BM 1910,729) and Allende (17 chondrules, BM 1981,M5) (Table 1). Both meteorites belong to the CV_{ox} group and are of petrologic type 3.6 [*Bonal et al.*, 2006]. Peak metamorphic temperatures are reported at around 330°C [*Bonal et al.*, 2006], resulting in minor redistribution of some mobile elements between the chondrules and matrix [*Bland et al.*, 2005; *Hezel et al.*, 2010]. Less mobile elements are not thought to have been affected [*Bland et al.*, 2005; *Hezel and Palme*, 2010]. The chondrules were extracted from the matrix by gentle mechanical crushing using a small hammer. The chondrules were then handpicked using a binocular microscope and further studied using an electron microscope (Figure 1). The mass of the chondrules studied in this paper varied between 0.2 and 2.47 mg, with diameters <1 mm. The electron microscope studies showed that chondrules were generally free of any attaching matrix to an extent to which it

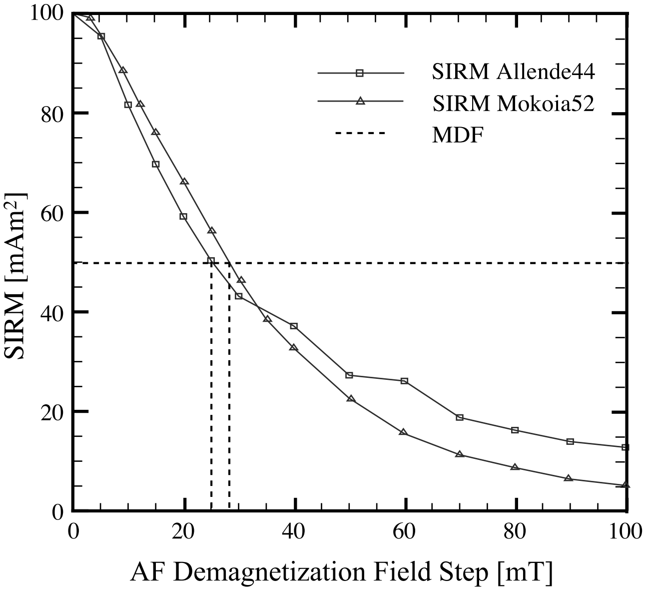

Figure 3. Examples of SIRM AF demagnetization curves for Allende and Mokoia. The MDF for SIRM of Allende44 is 25 mT and 28 mT for Mokoia52.

would not dominate the magnetic signal (Figure 1). Micro-CT studies *Hezel et al.* [2010] revealed metal and sulphide abundances in Allende between 0.0 and 0.6 vol% and in Mokoia between 0.9 and 11.8 vol%. The micro-CT technique is currently not developed to distinguish between metal and sulphide. For reference, we also investigated matrix and bulk samples from the two chondrites (Table 1).

[9] To characterize and quantify the magnetic properties and history of the chondrules we undertook a range of non-destructive experiments. In addition, estimates of the recorded paleointensity using the REMc method [*Acton et al.*, 2007] and the Preisach method [*Muxworthy and Heslop*, 2011] were made.

[10] First the natural remanent magnetization (NRM) was analyzed by demagnetizing the samples using AF demagnetization. For the samples with stronger NRM this was conducted using a combination of an Agico JR5A spinner magnetometer and a Molspin tumbling AF demagnetizer at Imperial College, London. The other samples were analyzed using 2G SQUID magnetometers with in-built AF demagnetization coils at the Helmholtz Centre Potsdam, Germany, and at the University of Oxford, UK. The Oxford SQUID was more sensitive ($\sim 2 \times 10^{-11}$ Am^2) than the Potsdam SQUID due to its narrower measuring chamber. The samples were induced with a saturating isothermal remanence (SIRM) and AF demagnetized; the combination of the NRM and SIRM AF demagnetization data is required for the REMc protocol [*Acton et al.*, 2007].

[11] For further magnetic characterization, magnetic hysteresis was measured on a Princeton Measurements Co. Alternating Gradient Magnetometer (AGM) at the Helmholtz Centre, Potsdam. In addition, backfield curves were measured to determine the 'standard' hysteresis parameters: coercive force (H_c), coercivity of remanence (H_{cr}), saturation magnetization (M_s), and saturation of remanence (M_{rs}), commonly plotted as ratios on the "Day plot" [*Day et al.*, 1977]. Partial hysteresis curves used to construct FORC distributions [*Roberts et al.*, 2000] were measured using the AGM for (1) basic magnetic characterization purposes and (2) for paleointensity estimations using the Preisach-based method of *Muxworthy and Heslop* [2011]. FORC distributions yield information about the coercivity distribution (H_c) and magnetic interactions (H_u) within a sample. Isothermal remanent magnetization (IRM) acquisition curves were also measured using the AGM for remanent coercivity spectra analysis [*Heslop et al.*, 2002].

3. Results

3.1. Original NRM and NRM Demagnetization

[12] The range of original NRM intensities of Mokoia chondrules was 0.1–67 mAm^{2}kg^{-1} with a median of 1.2 mAm^{2}kg^{-1} (Table 1). The median is similar to the Mokoia matrix NRM of 1.2 mAm^{2}kg^{-1} and the original NRM of the Mokoia bulk sample is 10.6 mAm^{2}kg^{-1}. The NRM intensity of the Allende chondrules ranged between 0.1–3.7 mAm^{2}kg^{-1}, the two matrix samples had values of 1.2 and 1.7 mAm^{2}kg^{-1} and the bulk NRM was 0.3 mAm^{2}kg^{-1}. The original NRM range for Mokoia and Allende are within the same ranges reported by *Gattacceca and Rochette* [2004] and *Acton et al.* [2007], and with the exception of two chondrules we also observe that the matrix has a much stronger NRM per unit mass than the chondrules (at least double) for Allende as reported by *Nagata and Funaki* [1983]. Typical NRM AF demagnetization data are plotted as orthogonal projection (Zijderveld) plots (Figure 2). Most Mokoia and Allende chondrules (Figures 2a, 2b, 2c, and 2d) and bulk samples (Figures 2e and 2f) showed two or more component magnetizations. Some of the secondary magnetizations were removed at relatively low AF fields, suggesting that their origin may be shock related (e.g., Figure 2b). Typically shock magnetization associated with low-impact pressures is relatively magnetically soft [*Gattacceca et al.*, 2007, 2010]. Both the NRM AF demagnetization decay curves and the paleomagnetic directions were observed to be typically more stable in the Mokoia samples than the Allende samples during AF demagnetization. The samples were not orientated with respect to one another.

3.2. SIRM and SIRM Demagnetization

[13] The SIRM gives a rough estimate of the amount of remanence carrying magnetic minerals within a sample; i.e., it is a measure of magnetic concentration, though it is also affected by magnetic mineralogy and grain size. A large range of SIRM values were identified within each meteorites chondrules, between 7.0–1050 mAm^{2}kg^{-1} for Mokoia and 1.4–105 mAm^{2}kg^{-1} for Allende (Figures 3 and 4 and Table 1). The range of SIRMs for Allende chondrules are within the SIRM estimates of *Acton et al.* [2007] (Figure 4). The Mokoia chondrules have a median SIRM of 58 mAm^{2}kg^{-1} compared to 21 mAm^{2}kg^{-1} for Allende. The Mokoia matrix (354 mAm^{2}kg^{-1}) and bulk (983 mAm^{2}kg^{-1}) samples also have higher SIRM values than the Allende bulk (61 mAm^{2}kg^{-1}) and matrix (121 mAm^{2}kg^{-1} and 1.4 mAm^{2}kg^{-1}). The AF demagnetization curves for the SIRM were magnetically harder than the NRM AF demagnetization curves and on average the MDF for the Mokoia chondrules were typically between 25 and 30 mT and 25 mT for Allende (Table 1).

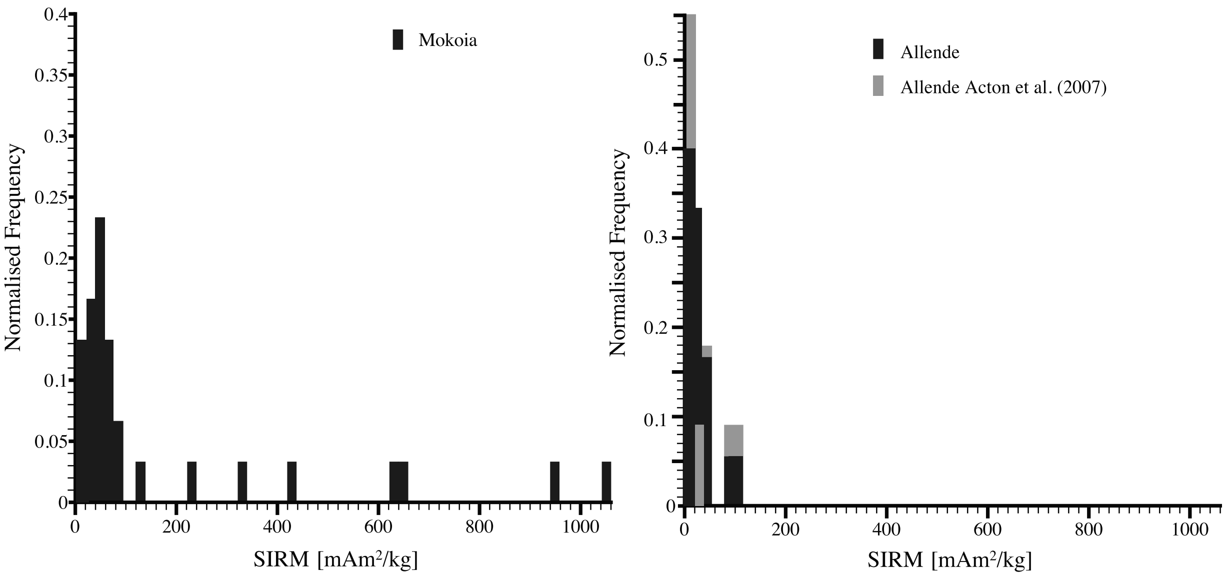

Figure 4. Normalized SIRM data for the Allende and Mokoia chondrules. Allende chondrules all have SIRM < 105 mAm^2kg^{-1} with nearly 75% <40 mAm^2kg^{-1}. *Acton et al.*'s [2007] Allende SIRM results have been included for comparison. Mokoia has much more variability from 7 to 1050 mAm^2kg^{-1} with only 25% <40 mAm^2kg^{-1} and nearly 70% <100 mAm^2kg^{-1}.

3.3. Magnetic Hysteresis

[14] The magnetic hysteresis parameters for the samples are tabulated in Table 1. The Mokoia chondrules and matrix plot within the PSD region of the Day plot (Figure 5), toward the SD area indicating the Mokoia samples are more likely to carry a stable remanence than the Allende chondrules and matrix that plot toward the PSD/MD boundary. Samples Mokoia87 and Mokoia89 were diamagnetic. The

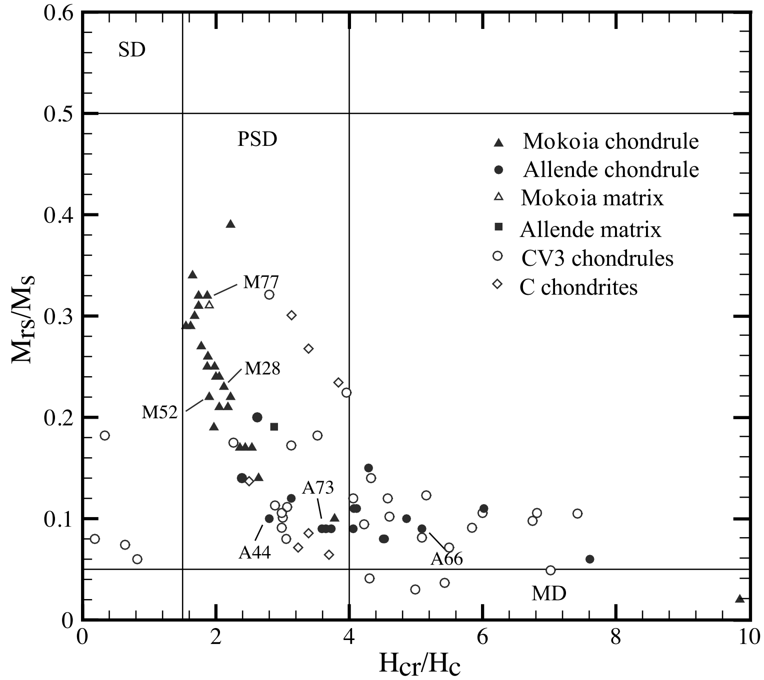

Figure 5. A "Day" plot [*Day et al.*, 1977] represents the ratios of the hysteresis parameters M_{rs}/M_s versus H_{cr}/H_c for chondrules from the two meteorites. The areas are split into SD, PSD, and MD behavior. Mokoia chondrules reside mainly near the SD/PSD boundary, whereas the Allende chondrules plot much closer to the PSD/MD boundary. CV3 chondrules and C chondrite results from previous studies [*Nagata*, 1979; *Sugiura et al.*, 1979; *Wasilewski*, 1981; *Acton et al.*, 2007] are used for comparison. Representative chondrules in Figures 2 and 4 are highlighted for reference.

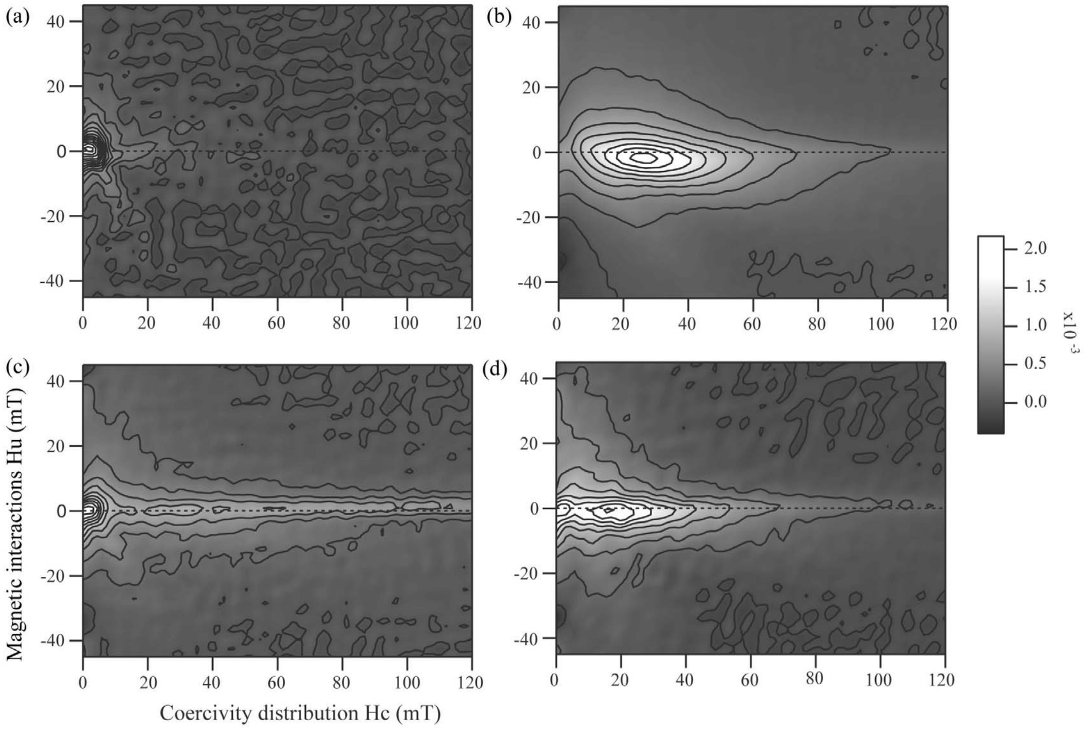

Figure 6. Representative FORC diagrams for Allende and Mokoia chondrules, displaying the three classifications discussed in the text: (a) type A, Allende-like (Allende66); (b) type M, Mokoia-like (Mokoia77); and (c) type A_1 (Allende73). Some samples displayed a combination of types A and M behavior as seen in (d) sample Allende44. In all the figures, the smoothing factor was three and the averaging time was 100 ms.

Mokoia chondrules generally have higher coercivities, indicating finer grain sizes for the magnetic minerals (Table 1 and Figure 5). CV3 chondrules and carbonaceous chondrites from other studies have been included in Figure 5 [*Nagata*, 1979; *Sugiura et al.*, 1979; *Wasilewski*, 1981; *Acton et al.*, 2007].

[15] FORC distributions [e.g., *Roberts et al.*, 2000; *Muxworthy and Roberts*, 2007] were also measured and representative plots are shown in Figure 6. As a first-order interpretation of a FORC diagram, the vertical axis (h_u) represents magnetic interactions within a sample and the horizontal axis (h_c) approximates the coercivity distribution. In the absence of any interactions, the coercivity distribution is a ridge along the zero interactions axis ($h_u = 0$). The series of FORCs were processed using FORCinel [*Harrison and Feinberg*, 2008]. In a similar fashion to *Acton et al.* [2007] we split the FORC diagrams' characteristics into two classification types: A and M (Figure 6 and Table 1). Most Allende chondrules were type A (Figure 6a); these are typified by low-field coercivity distributions with little or no spreading along the h_u axis. These are consistent with FORC diagrams for samples displaying PSD behavior [*Muxworthy and Dunlop*, 2002] and are similar to the type A FORC distributions recorded by *Acton et al.* [2007]. Some Allende chondrules also displayed a main peak at low-coercive forces close to the h_c axis, but with distribution tails extending to high coercivities beyond 60 mT (Type A_1) (Figure 6c). Type A and A_1 Allende samples are similar in terms of FORC characteristics, to the Allende chondrules measured by *Acton et al.* [2007]. The Mokoia chondrules displayed pre-dominantly type M behavior (Figure 6b), typified by oval distributions with the main peak away from the origin between 10 and 40 mT. Type M distributions display evidence for magnetic interactions below 20 mT, the degree of interactions decreasing for larger h_c values (Figure 6b). This probably reflects the increasing dominance of the intrinsic anisotropy over magnetic interactions with increasing coercivity [*Muxworthy et al.*, 2004]. The FORC distribution also has a negative region near the h_u axis in the lower half of the FORC diagram. This is typical of uniaxial SD behavior [*Carvallo et al.*, 2006]. Some Allende and Mokoia chondrules display a mixed composite of the type A and M distributions, displaying two peaks; e.g., Mokoia35 and Allende44 (Figure 6d). *Acton et al.* [2007] showed no FORC diagrams like Mokoia as described above but did show one Allende sample similar to our A and M composite. The only matrix sample able to be measured was the Mokoia matrix, its FORC distribution was type M.

3.4. IRM Acquisition Analysis

[16] Typical IRM acquisition curves and distributions are shown in Figure 7. The latter represents the distribution of the remanent coercivities, which is related to grain size and magnetic mineralogy. The Allende chondrules typically display a wide remanent coercivity distribution with no clearly defined main peak (Figure 7a). Mokoia chondrules

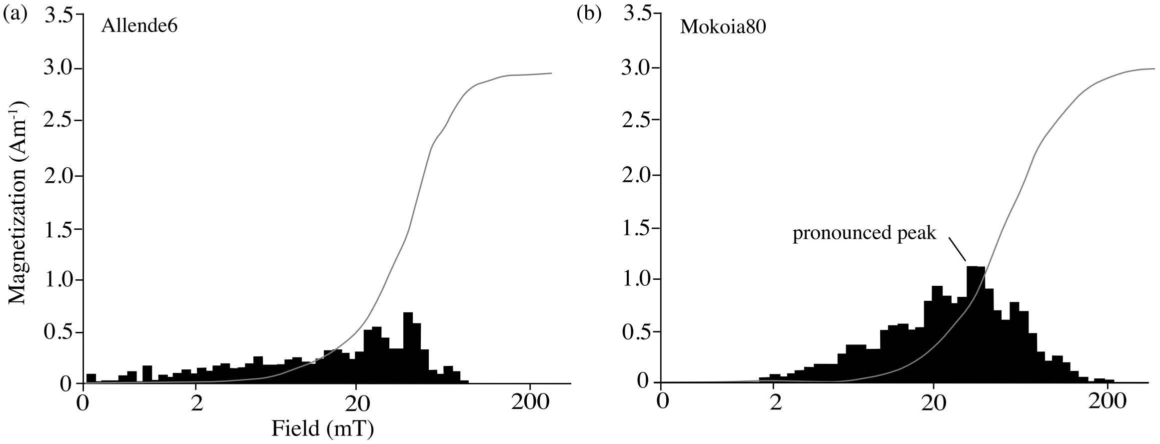

Figure 7. IRM acquisition curves and their acquisition distributions. (a) Allende6, typical Allende chondrule IRM curve with a wide distribution and no main peak coercivity, and (b) Mokoia80, typical Mokoia chondrule IRM curve with a possible single coercivity peak in the distribution.

typically display coercivity distribution with one clear peak (Figure 7b) indicating a possible prominent magnetic mineral contributing to the magnetic signal with the exception of one sample Mokoia88 (Table 1).

4. Discussion

[17] Mokoia's chondrules, matrix, and bulk show similar results for NRM, SIRM, FORC distributions, and grain sizes; in contrast, the Allende meteorite displayed greater variation between the three components, the bulk revealed NRM and SIRM data closer to the chondrule results than the matrix (Table 1). A detailed discussion of the results, magnetic mineralogy, and paleointensity estimates follows.

4.1. Magnetic Relationship Between Chondrules, Matrix and Bulk

[18] The Mokoia chondrules display more SD-like characteristics, indicating the magnetic particles within the chondrules are smaller than in the Allende chondrules. The Mokoia matrix displays similar properties to the Mokoia chondrules; e.g., a median NRM for both the Mokoia chondrules and matrix of 1.2 mAm^2kg^{-1}. The SIRM for the Mokoia matrix (354 mAm^2kg^{-1}) is also within the range observed for Mokoia chondrules 7.0–1050 mAm^2kg^{-1} and both the Mokoia matrix and chondrules have similar hysteresis parameters (Table 1 and Figure 3) and FORC distributions (Table 1). The Mokoia bulk sample has NRM and SIRM intensities similar to the chondrule values. These results suggest that the Mokoia matrix and bulk samples could have similar magnetic mineralogy to the chondrules, which may be due to a common source.

[19] The two Allende matrix samples are significantly different from one another, with SIRM values of 1.4 and 121 mAm^2kg^{-1}, and are at the extremes of the Allende chondrule range 1.4–105 mAm^2kg^{-1} (Table 1). There is either a significant heterogeneity within the Allende matrix or one sample has a non-representative amount of magnetic minerals. The Allende matrix samples also had s stronger NRM per unit mass than the chondrules (Table 1) (with the exception of two chondrules) as reported by *Nagata and Funaki* [1983].

4.2. IRM Analysis of Chondrules With Interpretation of Magnetic Mineralogy

[20] To further quantify the magnetic mineralogy, we analyzed the IRM acquisition data using the IRM unmixing algorithm of *Heslop and Dillon* [2007]. This program performs a linear unmixing of remanence data into end-members (EM) based on coercivities, using a nonnegative matrix factorization algorithm. The algorithm makes no assumptions about distribution shape. The number of end-members selected is based upon the significance level and the algorithm's ability to separate the signal into its contributing components likely to be representing individual minerals.

[21] For both the Mokoia chondrules and Allende chondrules three end-members (EM) with significance levels above 0.990 were identified (Figure 8). The three Allende chondrule EMs contribute at 42%, 32%, and 26% to the bulk signal with coercivity peaks at 9.7 mT (Figure 8a) and 46 mT (Figure 8b) identified with the first two EMs. No clear coercivity peak was identified for the third EM (Figure 8c). The three Mokoia chondrule EMs were weighted at 48%, 37%, and 15% of the total signal, with coercivity peaks at 9.7 mT for EM1 (Figure 8d), and 17 mT and 22 mT for EM2 (Figure 8e). No clear coercivity peak was identified for EM3 (Figure 8f). A Kolmogorov-Smirnov test was conducted and a commonality between the two sets of end-members for the two meteorites exists at a 95% confidence level. The end-members with the highest component for both meteorites have the same peak coercivity (9.7 mT) (Figures 8a and 8d). We base the following mineralogical interpretation of the magnetic data with the aid of the literature, which usually claims that there are FeNi, pyrrhotite, and magnetite phases [e.g., *Banerjee and Hargraves*, 1972; *Nagata and Funaki*, 1983; *Zanda*, 2004; *Hezel et al.*, 2008; *Weiss et al.*, 2010]. The low-coercivity mineral is possibly the same mineral phase in each meteorite and is likely to be multidomain FeNi: taenite, kamacite and/or awaruite, Allende's second end-member with a high-coercivity peak at 46 mT probably reflects the iron sulphide phase (pyrrhotite) (Figures 1 and 8b) and Mokoia's second end-member with a coercivity peak at 17 mT is likely to be magnetite (Figure 8e). Given the reported abundance of magnetite in Mokoia [*Krot et al.*,

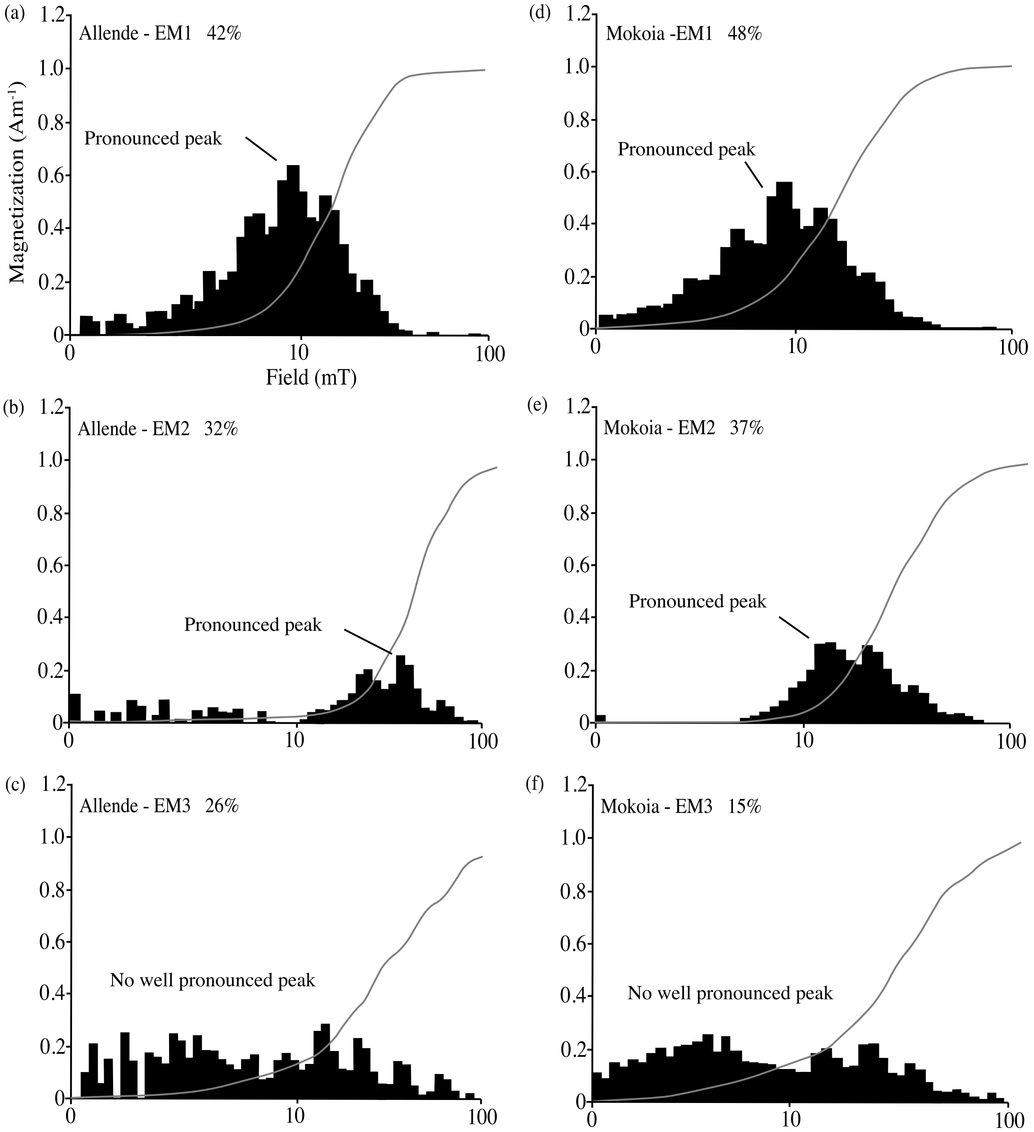

Figure 8. The IRM analysis end-member distributions. Allende chondrules have three end-members with different peak coercivities and abundances within the chondrules: (a) EM1 = 42%, (b) EM2 = 32%, and (c) EM3 = 26%. Mokoia chondrules have three end-members: (d) EM1 = 48%, (e) EM2 = 37%, and (f) EM3 = 15%. Suggested magnetic mineralogy for coercivity peaks at 9.7 mT = NiFe (awaruite, kamacite, and/or taenite), 17 mT = magnetite, and 45 mT = iron sulphide (pyrrhotite).

2005], and the similarity between EM1 (Figure 8d) and EM2 (Figure 8e) it could be argued that they represent magnetite and FeNi respectively instead. Allende is also known to contain magnetite [*Wasilewski and Saralker*, 1981; *Rubin*, 1991; *Bland et al.*, 2004], but as a minor phase [*Wasilewski*, 1981]. It is possible that the poorly defined EM3 (26%) (Figure 8c) is representative of magnetite in Allende, but no direct detection of magnetic minerals were made in this study, as it was not possible to heat the samples to determine their Curie temperatures.

4.3. Paleointensity Estimates

[22] Previous paleofield intensity estimates for carbonaceous chondrites using a variety of techniques, indicate a range of intensities generally between 0.2 and 110 μT. Several magnetic studies have been conducted on the Allende meteorite [e.g., *Banerjee and Hargraves*, 1972; *Lanoix et al.*, 1978; *Acton et al.*, 2007], but data on the Mokoia meteorite is limited [*Brecher and Arrhenius*, 1974; *Stacey*, 1976]. Two methods were adopted to calculate paleointensities in this study: (1) the REMc method [*Acton et al.*, 2007] and (2) the recent Preisach method [*Muxworthy and Heslop*, 2011; *Muxworthy et al.*, 2011]. Both methods assume that the NRM is a thermoremanence in origin. The REMc estimates were made using the NRM and SIRM AF demagnetization data alone, while the Preisach method combines the FORC distribution data with the NRM AF demagnetization data and the SIRM.

4.3.1. REMc Paleointensity Estimates

[23] Following the procedure outlined by *Acton et al.* [2007], we used the Zijderveld plots (Figure 2) to select the range of NRM and SIRM AF demagnetization data to estimate the

Table 2. The Paleointensity Results From This Study

Meteorite	REMc (μT)	Preisach (μT)
Allende	29[a] (19–39)	21[b] (3–39)
Mokoia	44[c] (24–64)	31[d] (9–53)

[a] Average of 12.
[b] Average of 7.
[c] Average of 17.
[d] Average of 11.

paleointensity. The REMc paleointensity estimates are made by identifying an AF demagnetization range for which the NRM/SIRM ratio is relatively constant (ChRM in Table 1), averaging this NRM/SIRM ratio and multiplying it by 3000 to yield an estimate in micro-Tesla [*Acton et al.*, 2007]. As discussed by *Acton et al.* [2007] and *Gattacceca and Rochette* [2004], it is important to identify the correct NRM/SIRM ratio interval to try and identify any primary magnetization and not overprinting (Figure 2). The estimates for the Mokoia chondrules range from 3–140 μT and for the Allende chondrules from 13–60 μT (Table 1). The large spread of data may be due to (1) non-ideal recording behavior of the chondrules, (2) a range of magnetic field intensities experienced by the chondrules on formation, or (3) within the error margins of the method. Many of the NRM demagnetization curves were of too low a quality due to noise, to determine consistent REMc method estimates. The REMc method has been shown to be more reliable than REM' or REM on Allende chondrules [*Acton et al.*, 2007].

[24] We take the arithmetic mean paleointensity estimate for each meteorite and determine a 95% confidence range (CI_{95}) (Table 2). In doing this we are assuming that the chondrules experience the same magnetic field during acquisition. The mean REMc estimates for Mokoia and Allende are 44 μT (CI_{95} 24–64 μT) and 29 μT (CI_{95} 19–39 μT) respectively (Table 2). Both paleointensities are within the range of previous estimates for carbonaceous chondrites (0.2–110 μT) [e.g., *Banerjee and Hargraves*, 1972; *Gattacceca and Rochette*, 2004; *Acton et al.*, 2007] and the two meteorites show a difference of 15 μT.

4.3.2. Preisach Paleointensity Estimates

[25] We used the Preisach method described by *Muxworthy and Heslop* [2011] to determine paleointensity estimates from the measured FORC data. The method works by using the room temperature-measured FORC diagram to generate a Preisach distribution. Using thermally activated Preisach theory, the response of the Preisach distribution to simulated TRM acquisition is used to predict TRM/SIRM ratios as a function of applied field intensity. Comparing the predicted TRM/SIRM ratios with the measured NRM/SIRM ratios is then used to determine the paleointensity. In a similar manner to the REMc procedure of *Acton et al.* [2007], to allow for multicomponent magnetizations the Preisach method determines a paleofield estimate for each step of the NRM AF demagnetization data (Figure 2). Due to instrumental noise, some samples failed to yield reliable estimates.

[26] This method generated a range of field estimates; the Allende and Mokoia paleofield estimates were between 3–56 μT and 1–110 μT respectively (Table 1). This variability could be due to noise limitations as well as real variability. The average paleointensities were 21 μT (CI_{95} 3–39 μT) and 31 μT (CI_{95} 9–53 μT) for Allende and Mokoia, respectively (Table 2). The average intensities have a difference of 10 μT.

4.3.3. Comparison of the Two Sets of Paleointensity Estimates

[27] The REMc paleointensity method typically yields higher field estimates than the Preisach protocol (Figure 9 and Tables 1 and 2). For samples used in both methods the mean values were: (1) for Allende 22 and 21 μT for the REMc and Preisach methods, respectively, and (2) similarly for Mokoia 47 and 31 μT. *Muxworthy et al.* [2011] found for historical lavas that the REM method yielded consistently higher estimates for the paleointensity estimate (50% or higher) than the Preisach method, with significantly higher variation. *Muxworthy et al.* [2011] suggested the lower estimates determined using the Preisach protocol is more reliable than REM-type paleointensity estimates. There are several possible sources of uncertainty such as the NRM not being a thermoremanence in origin and the possibility that the magnetic minerals have not reliably recorded the magnetic field intensity due to multidomain character or non-unidirectional magnetization giving rise to the systematic errors in the paleointensity estimates (Figure 9). It is also likely that the chondrules were spinning during the acquisition of a TRM; rapidly rotating chondrules would acquire their net remanence along the rotation axis. For a suite of chondrules, the paleofield intensity data would be expected to display a cosine function distribution of intensities. Generally, shock induced remanent magnetizations which maybe present, are magnetically soft [*Gattacceca et al.*, 2007, 2010]; i.e., they are removed by low-AF demagnetization fields and are not used in the paleointensity determinations. The mineralogical exception is pyrrhotite, which is completely demagnetized at relatively low pressures (2.8 GPa [*Rochette et al.*, 2001]). Pyrrhotite is thought to be present in the Allende samples. If Allende chondrules experienced pressures greater than 2.8 GPa then depending on the magnetic fields present at the time, the resulting paleointensity estimates from both methods may be incorrect.

[28] The results from this study are unique for the Mokoia meteorite and add to the database of information already accumulated on Allende chondrules. Paleointensity results from this study are within the range observed in previous estimates, though comparing the results from this paper with the non-heating paleointensity estimates [e.g., *Acton et al.*, 2007] it is clear that the estimates from both the REMc and the Preisach protocols are slightly higher than those reported in recent literature [e.g., *Wasilewski and Dickinson*, 2000; *Acton et al.*, 2007; *Carporzen et al.*, 2011].

4.4. Origin of the Magnetization

[29] An important question is whether the recorded magnetization is primary, (i.e., pre-accretion) or secondary (i.e., post-accretion). There is some evidence in the literature that suggests the Allende chondrules carry a high-temperature component of remanence that maybe primary in origin [*Sugiura et al.*, 1979; *Sugiura and Strangway*, 1985; *Acton et al.*, 2007], though there is some evidence now to suggest secondary remanence [e.g., *Weiss et al.*, 2010].

[30] If magnetization is pre-accretionary it could be expected that we would observe a range of recorded magnetic field intensities due to inhomogeneities in the ambient magnetic field at the time of chondrule formation, though there is some

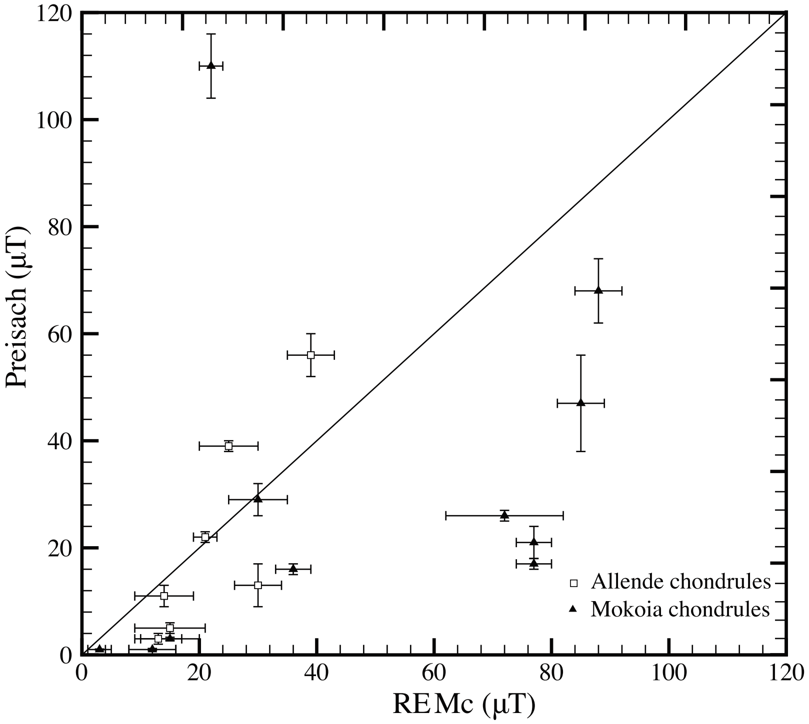

Figure 9. A comparison of the paleointensity estimates of both sets of chondrules using the two methods, REMc and Preisach with their associated errors. In the REMc method, for each sample, each selected AF demagnetization step yields an intensity, which is then averaged to provide an arithmetic mean and standard deviation (the error bar). In the Preisach method, for each sample, the error is determined by calculating an error for each selected AF demagnetization step using a bootstrap approach, then by taking the weighted mean of these AF demagnetisation steps, which also provides a standard deviation (the error bar).

natural variation in the recorded intensities due to the imperfect recording capabilities of natural magnetic assemblages [*Muxworthy et al.*, 2011]. Although the errors associated with recovering paleofield intensities are large, the recording of differing field intensities will increase the variation, potentially dominating it. The REMc results displayed estimates between 13 and 60 μT and 3–140 μT for Allende and Mokoia, respectively. This shows significant variability within each meteorite with larger ranges seen in Mokoia. The same trend is also observed for the Preisach method results, though the absolute sizes of the ranges are slightly smaller; Allende and Mokoia ranged between 3 and 56 μT and 1–110 μT respectively. These are large variations when compared with paleointensities recovered from lavas via the same methods [*Muxworthy et al.*, 2011], indicating that chondrules are (1) either particularly poor recorders of the paleofield, (2) were chemically altered, or (3) they were exposed to heterogeneous magnetic fields in the solar nebula.

[31] Post-accretionary magnetizations could be induced by (1) re-heating of the samples (the magnetic properties of the carrier-mineral will be re-set if a magnetic field is present, or demagnetized if not); or (2) chemical alteration of the magnetic mineral or growth of new magnetic phases during a post-accretionary hydrothermal and/or metamorphic event (such events are more likely to homogenize a previously magnetically heterogeneous chondrule population). It would be expected that the range of intensities would be much smaller and an average paleointensity to be more informative. The REMc method gave average paleofields for Allende and Mokoia of 29 and 44 μT respectively with 15 μT difference. For the Preisach method, Allende and Mokoia chondrules produced paleofields of 21 and 31 μT, respectively, with an intensity difference of 10 μT. The magnetic properties including the IRM end-member analysis, suggests that there is some commonality in major magnetic mineralogy in the Allende and Mokoia chondrules, both possibly dominated by FeNi phases (Figure 8) and that the remanence is most likely secondary. Generally, though not always, chemical alteration of primary magnetic minerals leads to an increase in the magnetic hardness [*Davis and Evans*, 1976; *van Velzen and Zijderveld*, 1992]; the Mokoia chondrules typically have higher coercivities than Allende, this can be seen in the hysteresis parameters (Figure 5 and Table 2) and FORC diagrams (Figure 6). Mokoia chondrules also show similar properties as the matrix and bulk samples, supporting ideas in the literature [*Krot et al.*, 2005] that Mokoia as a whole is chemically altered.

5. Conclusions

[32] This study was conducted to evaluate the magnetic properties of two carbonaceous chondrites of the CV type, Mokoia and Allende. Mokoia chondrules showed higher magnetic stability, were magnetically stronger samples than Allende chondrules and identified aspects of secondary magnetization. Mokoia's chondrules, matrix, and bulk do

not differ greatly in terms of their NRM, SIRM, magnetic mineralogy, or grain sizes indicating possible alteration of the whole meteorite. In contrast, Allende chondrules displayed greater variation between chondrules, matrix, and bulk components, the bulk revealed NRM and SIRM data closer to the chondrule results; however, the two matrix samples were distinct, either indicating huge heterogeneity or the possibility of non-representative sampling (Table 1). The results of this study suggest that Allende chondrules are more likely to partially retain primary magnetizations recorded by PSD grains (Figures 5 and 6) predominantly characterized by a low-coercivity mineralogy; e.g., FeNi, (Figures 7 and 8 and Table 1) as well as what is suggested to be pyrrhotite, than Mokoia chondrules, which display a larger percentage of what are thought to be alteration minerals like magnetite (Figures 2a, 5, and 6 and Table 1). However, both meteorites show signs of chemical alteration suggesting that their magnetization is most probably post-accretional.

[33] Based on the potentially erroneous assumption that the NRM of the samples is a thermoremanence in origin, the average paleofield intensity results from this study were as follows; 21 and 29 μT for Allende chondrules from respectively the Preisach and REMc methods, and for the Mokoia chondrules 31 and 44 μT for the Preisach and REMc methods respectively. Comparing the two paleointensity methods, the REMc method was consistently higher than the Preisach predictions. The Preisach technique takes into account the level of interactions, which should yield a more precise paleointensity compared with the cross-calibrated REMc method [*Muxworthy and Heslop*, 2011; *Muxworthy et al.*, 2011]. The range of paleointensities observed were 13–60 μT and 3–140 μT for Allende and Mokoia chondrules, respectively, in the REMc method, while the Preisach method yielded ranges of 3–56 μT and 1–110 μT for Allende and Mokoia chondrules. There is no considerable difference in the estimated range of paleofield intensities determined for each meteorite using both methods. Taking into consideration the rock magnetic data and the palaeomagnetic intensities in our interpretation, we suggest that Mokoia chondrules carry a post-accretionary magnetization and although Allende has a higher potential than Mokoia to retain its primary magnetization it also shows significant signs of post-accretionary magnetization.

[34] **Acknowledgments.** We would like to thank Norbert Nowaczyk at the Helmholtz Centre Potsdam and Conall Mac Niocaill at the University of Oxford for use of their paleomagnetic facilities. This work was part funded by the Royal Society and PPARC/STFC.

References

Acton, G., Q. Z. Yin, K. L. Verosub, L. Jovane, A. Roth, B. Jacobsen, and D. S. Ebel (2007), Micromagnetic coercivity distributions and interactions in chondrules with implications for paleointensities of the early solar system, *J. Geophys. Res.*, *112*, B03S90, doi:10.1029/2006JB004655.

Banerjee, S. K. and R. B. Hargraves (1972), Natural remanent magnetizations of carbonaceous chondrites and the magnetic field in the early solar system. *Earth Planet. Sci. Lett.*, *17*, 110–119, doi:10.1016/0012-821X(72)90265-8.

Bland, P. A., G. Cressey, and O. N. Menzies (2004), Modal mineralogy of carbonaceous chondrites by X-ray diffraction and Mössbauer spectroscopy, *Meteorit. Planet. Sci.*, *39*(1), 3–16, doi:10.1111/j.1945-5100.2004.tb00046.x.

Bland, P. A., O. Alard, G. K. Benedix, A. T. Kearsley, O. N. Menzies, L. Watt, and N. W. Rogers (2005), Volatile fractionation in the early Solar System and chondrule/matrix complementarity, *Proc. Natl. Acad. Sci. U. S. A.*, *102*, 13,755–13,760, doi:10.1073/pnas.0501885102.

Bonal, L., E. Quirico, M. Bourot-Denise, and G. Montagnac (2006), Determination of the petrologic type of CV3 chondrites by Raman spectroscopy of included organic matter, *Geochim. Cosmochim. Acta*, *70*, 1849–1863, doi:10.1016/j.gca.2005.12.004.

Brearley, A. J., and R. H. Jones (1998), Chondritic meteorites, in *Planetary Materials*, *Rev. Mineral.*, vol. 36, edited by J. J. Papike, chap. 3, pp. 1–398, Mineral. Soc. of Am., Washington, D. C.

Brecher, A. (1977), Meteoritic magnetism: Implications for parent bodies of origin, in *Comets, Asteroid and Meteorites*, edited by A. H. Delsemme, pp. 415–427, Univ. Toledo Press, Toledo, Ohio.

Brecher, A., and G. Arrhenius (1974), The paleomagnetic record in carbonaceous chondrites: Natural remanence and magnetic properties, *J. Geophys. Res.*, *79*(14), 2081–2106, doi:10.1029/JB079i014p02081.

Butler, R. F. (1972), Natural remanent magnetisation and thermomagnetic properties of Allende meteorite. *Earth Planet. Sci. Lett.*, *17*(1), 120–128, doi:10.1016/0012-821X(72)90266-X.

Carporzen, L., B. P. Weiss, L. T. Elkins-Tanton, D. L. Shuster, D. Ebel, and J. Gattacceca (2011), Magnetic evidence for a partially differentiated carbonaceous chondrite parent body, *Proc. Natl. Acad. Sci. U. S. A.*, *108*(16), 6386–6389, doi:10.1073/pnas.1017165108.

Carvallo, C., A. R. Muxworthy, and D. J. Dunlop (2006), First-order reversal curve (FORC) diagrams of magnetic mixtures: Micromagnetic models and measurements, *Phys. Earth Planet. Inter.*, *154*(3–4), 308–322, doi:10.1016/j.pepi.2005.06.017.

Collinson, D. W. (1994), The magnetism of meteorites and early Solar System magnetic fields, *Philos. Trans. R. Soc. London A*, *349*(1690), 197–207.

Davis, P. M., and M. E. Evans (1976), Interacting single-domain properties of magnetite intergrowths, *J. Geophys. Res.*, *81*(5), 989–994, doi:10.1029/JB081i005p00989.

Day, R., M. Fuller, and V. A. Schmidt (1977), Hysteresis properties of titanomagnetites: Grain size and compositional dependence, *Phys. Earth Planet. Inter.*, *13*(4), 260–267, doi:10.1016/0031-9201(77)90108-X.

Donati, J. F., F. Paletou, J. Bouvier, and J. Ferreira (2005), Direct detection of a magnetic field in the innermost regions of an accretion disk, *Nature*, *438*, 466–469, doi:10.1038/nature04253.

Gattacceca, J., and P. Rochette (2004), Toward a robust normalized magnetic paleointensity method applied to meteorites, *Earth Planet. Sci. Lett.*, *227*, 377–393, doi:10.1016/j.epsl.2004.09.013.

Gattacceca, J., A. Lamali, P. Rochette, M. Boustie, and L. Berthe (2007), The effects of explosive-driven shocks on the natural remanent magnetization and the magnetic properties of rocks, *Phys. Earth Planet. Inter.*, *162*, 85–98, doi:10.1016/j.pepi.2007.03.006.

Gattacceca, J., L. Berthe, M. Boustie, F. Vadeboin, P. Rochette, and T. De Resseguier (2008), On the efficiency of shock magnetization processes, *Phys. Earth Planet. Inter.*, *166*, 1–10, doi:10.1016/j.pepi.2007.09.005.

Gattacceca, J., M. Boustie, E. Lima, B. P. Weiss, T. de Resseguier, and J. P. Cuq-Lelandais (2010), Unravelling the simultaneous shock magnetization and demagnetization of rocks, *Phys. Earth Planet. Inter.*, *182*, 42–49, doi:10.1016/j.pepi.2010.06.009.

Harrison, R. J., and J. M. Feinberg (2008), FORCinel: An improved algorithm for calculating first-order reversal curve distributions using locally weighted regression smoothing, *Geochem. Geophys. Geosyst.*, *9*, Q05016, doi:10.1029/2008GC001987.

Herndon, J., M. W. Rowe, E. E. Larson, and D. E. Watson (1976), Thermomagnetic analysis of meteorites; 3, C3 and C4 chondrites, *Earth Planet. Sci. Lett.*, *29*, 283–290, doi:10.1016/0012-821X(76)90132-1.

Heslop, D., and M. Dillon (2007), Unmixing magnetic remanence curves without a priori knowledge, *Geophys. J. Int.*, *170*(2), 556–566, doi:10.1111/j.1365-246X.2007.03432.x.

Heslop, D., M. J. Dekkers, P. P. Kruiver, and I. H. M. van Oorschot (2002), Analysis of isothermal remanent magnetization acquisition curves using the expectation-maximization algorithm, *Geophys. J. Int.*, *148*(1), 58–64, doi:10.1046/j.0956-540x.2001.01558.x.

Hezel, D. C., and H. Palme (2010), The chemical relationship between chondrules and matrix and the chondrule matrix complementarity, *Earth Planet. Sci. Lett.*, *294*, 85–93, doi:10.1016/j.epsl.2010.03.008.

Hezel, D. C., S. S. Russell, A. J. Ross, and A. T. Kearsley (2008), Modal abundances of CAIs: Implications for bulk chondrite element abundances and fractionations, *Meteorit. Planet. Sci.*, *43*(11), 1879–1894, doi:10.1111/j.1945-5100.2008.tb00649.x.

Hezel, D. C., A. W. Needham, R. Armytage, B. Georg, R. Abel, E. Kurahashi, B. J. Coles, M. Rehkämper, and S. S. Russell (2010), A nebula setting as the origin for bulk chondrule Fe isotope fractionations in CV chondrites, *Earth Planet. Sci. Lett.*, *296*, 423–433, doi:10.1016/j.epsl.2010.05.029.

Huss, G. R., C. M. O. Alexander, H. Palme, P. A. Bland, and J. T. Wasson (2005), Genetic relationships between chondrules, fine-grained rims, and interchondrule matrix, in *Chondrites and the Protoplanetary Disk*, edited by A. N. Krot, E. R. D. Scott, and B. Reipurth, *Astron. Soc. Pac. Conf. Ser.*, *341*, 701–731.

Jones, R. H., J. N. Grossman, and A. E. Rubin (2005), Chemical, mineralogical and isotopic properties of chondrules: Clues to their origin, in *Chondrites and the Protoplanetary Disk*, edited by A. N. Krot, E. R. D. Scott, and B. Reipurth, *Astron. Soc. Pac. Conf. Ser.*, *341*, 251–285.

Kletetschka, G., T. Kohout, and P. J. Wasilewski (2003), Magnetic remanence in the Murchison meteorite, *Meteorit. Planet. Sci.*, *38*(3), 399–405, doi:10.1111/j.1945-5100.2003.tb00275.x.

Krot, A. N., M. I. Petaev, E. R. D. Scott, B.-G. Choi, M. E. Zolensky, and K. Keil (1998), Progressive alteration in CV3 chondrites: More evidence for asteroidal alteration, *Meteorit. Planet. Sci.*, *33*(5), 1065–1085, doi:10.1111/j.1945-5100.1998.tb01713.x.

Krot, A. N., I. D. Hutcheon, A. J. Brearley, O. V. Pravdivtseva, M. I. Petaev, and C. M. Hohenberg (2005), Timescales and settings for alteration of chondritic meteorites, in *Meteorites and the Early Solar System II*, edited by D. S. Lauretta and H. Y. McSween Jr., pp. 525–553, Univ. of Ariz. Press, Tucson.

Lanoix, M., D. W. Strangway, and G. W. Pearce (1978), The primordial magnetic field in chondrules of the Allende meteorite, *Geophys. Res. Lett.*, *5*(1), 73–76, doi:10.1029/GL005i001p00073.

Muxworthy, A. R., and D. J. Dunlop (2002), First-order reversal curve (FORC) diagrams for pseudo-single-domain magnetites at high temperature, *Earth Planet. Sci. Lett.*, *203*, 369–382, doi:10.1016/S0012-821X(02)00880-4.

Muxworthy, A. R., and D. Heslop (2011), A Preisach methodology to determining absolute paleointensities: 1. Theoretical framework, *J. Geophys. Res.*, *116*, B04102, doi:10.1029/2010JB007843.

Muxworthy, A. R., and A. P. Roberts (2007), First-order reversal curve (FORC) diagrams, in *Encyclopedia of Geomagnetism and Paleomagnetism*, edited by D. Gubbins and E. Herrero-Bervera, pp. 266–272, Springer, Dordrecht, Netherlands.

Muxworthy, A. R., D. Heslop, and W. Williams (2004), Influence of magnetostatic interactions on first-order-reversal-curve (FORC) diagrams: A micromagnetic approach, *Geophys. J. Int.*, *158*, 888–897, doi:10.1111/j.1365-246X.2004.02358.x.

Muxworthy, A. R., D. Heslop, G. A. Paterson, and D. Michalk (2011), A Preisach methodology to determining absolute paleointensities: 2. Field testing, *J. Geophys. Res.*, *116*, B04103, doi:10.1029/2010JB007844.

Nagata, T. (1979), Meteorite magnetism and the early solar system magnetic field, *Phys. Earth Planet. Inter.*, *20*, 324–341, doi:10.1016/0031-9201(79)90055-4.

Nagata, T., and M. Funaki (1983), Paleointensity of the Allende carbonaceous chondrite, *Mem. Natl. Inst. Polar Res, Spec. Issue 30*, 403–434.

Nakamura, T., K. Tomeoka, T. Sekine, and H. Takeda (1995), Impact induced chondrule flattening in the Allende CV3 carbonaceous chondrite: Shock experiments, *Meteoritics*, *30*, 344–347.

Preisach, F. (1935), Über die magnetische Nachwirkung, *Z. Phys.*, *94*, 277–302, doi:10.1007/BF01349418.

Roberts, A. P., C. R. Pike, and K. L. Verosub (2000), First-order reversal curve diagrams: A new tool for characterizing the magnetic properties of natural samples, *J. Geophys. Res.*, *105*(B12), 28,461–28,475, doi:10.1029/2000JB900326.

Rochette, P., J.-P. Lorand, G. Fillion, and V. Sautter (2001), Pyrrhotite and the remanent magnetization of SNC meteorites: A changing perspective on Martian magnetism, *Earth Planet. Sci. Lett.*, *190*, 1–12, doi:10.1016/S0012-821X(01)00373-9.

Rubin, A. E. (1991), Euhedral awaruite in the Allende meteorite: Implications for the origin of awaruite and magnetite-bearing nodules in CV3 chondrites, *Am. Mineral.*, *76*, 1356–1362.

Scott, E. R. D., K. Keil, and D. Stöffler (1991), Impact heating of shocked chondrites, *Meteoritics*, *26*, 393.

Scott, E. R. D., K. Keil, and D. Stöffler (1992), Shock metamorphism of carbonaceous chondrites, *Geochim. Cosmochim. Acta*, *56*, 4281–4293, doi:10.1016/0016-7037(92)90268-N.

Sears, D. W. G. (2004), *The Origin of Chondrules and Chondrites*, Cambridge Univ. Press, Cambridge, U. K., doi:10.1017/CBO9780511536137.

Stacey, F. D. (1976), Palaeomagnetism of meteorites, *Annu. Rev. Earth Planet. Sci.*, *4*, 147–157, doi:10.1146/annurev.ea.04.050176.001051.

Stöffler, D., K. Keil, and E. R. D. Scott (1991a), Shock metamorphism of ordinary chondrites, *Geochim. Cosmochim. Acta*, *55*, 3845–3867, doi:10.1016/0016-7037(91)90078-J.

Stöffler, D., K. Keil, and E. R. D. Scott (1991b), Proposal for a revised petrographic shock classification of chondrites, *Meteoritics*, *26*, 398.

Sugiura, N., and D. W. Strangway (1985), NRM directions around a centimetre-sized dark inclusion in Allende, *Proc. Lunar Planet. Sci. Conf. 15th*, Part 2, *J. Geophys. Res.*, *90*, suppl., C729–C738.

Sugiura, N., M. Lanoix, and D. W. Strangway (1979), Magnetic fields of the Solar Nebula as recorded in chondrules from the Allende meteorite, *Phys. Earth Planet. Inter.*, *20*(2–4), 342–349, doi:10.1016/0031-9201(79)90056-6.

Thellier, E., and O. Thellier (1959), Sur l'intensité du champ magnétique terrestre dans le passé historique et géologique, *Ann. Geophys.*, *15*, 285–376.

van Velzen, A. J., and J. D. A. Zijderveld (1992), A method to study alterations of magnetic minerals during thermal demagnetization applied to a fine-grained marine marl (Trubi formation, Sicily), *Geophys. J. Int.*, *110*, 79–90, doi:10.1111/j.1365-246X.1992.tb00715.x.

Wasilewski, P. (1981), New magnetic results from Allende C3(V), *Phys. Earth Planet. Inter.*, *26*(1–2), 134–148, doi:10.1016/0031-9201(81)90105-9.

Wasilewski, P. J., and T. Dickinson (2000), Aspects of the validation of magnetic remanence in meteorites, *Meteorit. Planet. Sci.*, *35*, 537–544, doi:10.1111/j.1945-5100.2000.tb01434.x.

Wasilewski, P. J., and C. Saralker (1981), Stable NRM and mineralogy in Allende: Chondrules. *Proc. Lunar Planet. Sci. Conf.*, *12*, 1217–1227.

Weiss, B. P., L. Carporzen, L. T. Elkins-Tanton, and D. S. Ebel (2009), Evidence for internally generated magnetic fields in CV chondrite parent planetismal, *Proc. Lunar Planet. Sci. Conf.*, *40*, 2237.

Weiss, B. P., J. Gattacceca, S. Stanley, P. Rochette, and U. R. Christensen (2010), Paleomagnetic records of meteorites and early planetesimal differentiation, *Space Sci. Rev.*, *152*(1–4), 341–390, doi:10.1007/s11214-009-9580-z.

Westphal, M. (1986), Natural remanent magnetization, thermoremanent magnetization and reliability of paleointensity determinations on H chondrites, *Phys. Earth Planet. Inter.*, *43*, 300–306, doi:10.1016/0031-9201(86)90019-1.

Yu, Y. (2006), How accurate can NRM/SIRM determine the ancient planetary magnetic field intensity?, *Earth Planet. Sci. Lett.*, *250*, 27–37, doi:10.1016/j.epsl.2006.07.027.

Yu, Y., S.-J. Doh, W. Kim, and K. Min (2009), Ancient stable magnetism of the Richardton H5 chondrite, *Phys. Earth Planet. Inter.*, *177*, 12–18, doi:10.1016/j.pepi.2009.07.003.

Zanda, B. (2004), Chondrules, *Earth Planet. Sci. Lett.*, *224*, 1–17, doi:10.1016/j.epsl.2004.05.005.

P. A. Bland and D. C. Hezel, Impacts and Astromaterials Research Centre, Department of Mineralogy, Natural History Museum, Cromwell Road, London SW7 5BD, UK.

S. Emmerton and A. R. Muxworthy, Impacts and Astromaterials Research Centre, Department of Earth Science and Engineering, Imperial College London, South Kensington Campus, Prince Consort Road, London SW7 2AZ, UK. (stacey.emmerton05@imperial.ac.uk)